

Layer-by-Layer Design of Bianisotropic Metamaterial and Its Homogenization

Liang Peng^{1,*}, Xiaoxiao Zheng¹, Kewen Wang¹, Shuaifei Sang¹,
Yuntian Chen², and Gaofeng Wang¹

Abstract—In this paper, we study the design and homogenization of bianisotropic metamaterials originated from planar split-ring resonators, which would potentially meet the requirements of the emerging photonic topological insulators and some other types of exotic photonic materials with non-trivial states. We show that the off-diagonal elements in the magneto-electric tensor can be realized by combining the planar split-ring resonators with different orientations. To ease the fabrication process, a layer-by-layer design of metamaterials with desired bianisotropy is proposed. The design and homogenization procedure of such metamaterials are verified through effective parameter retrieval approach and computer based simulation. With the proposed structure, the complex magneto-electric coupling is realized in layered structures through planar techniques, which may be useful in the terahertz and optical range.

1. INTRODUCTION

Artificial electromagnetic (EM) metamaterial (MM), which could be engineered by tuning its composing constituents and may be described by effective constitutives [1], has attracted lots of attention in the past decade. According to MM fundamentals, the effective parameters of the MMs are mainly determined by the resonance of the unit structures [2, 3]. Consequently, plasmon-like dispersion may be observed in both the effective permittivity and the effective permeability, which gives rise to many interesting EM phenomena, such as backward waves, negative refraction, reversed Doppler effect and etc. [4]. With peculiar EM properties, the MMs are applied in inventing novel devices with revolutionary features, e.g., the flat lenses with perfect imaging and super resolution [5], the transformation optics devices and the invisible cloaks [6, 7].

In recent years, it is reported that bianisotropic materials show their particular capability in constructing the pseudo-spin states [8, 9], such that the emulation of topological insulators in photonics (or photonic topological insulators) may be possible. With the photonic topological insulators (PTIs), the transportation of EM power without any backward scattering/dissipation is expected, because of their non-trivial features. Taking advantage of micro/nano fabrication and recent developments in MMs, PTIs would be realizable by carefully designing the unit cell structures [8, 10]. Besides, it is worth to mention that the bianisotropic materials are considered as a good candidate to identify the circular polarized waves without applying additional detecting probes [10]. Further more, waveguides filled with bianisotropic materials can be used to realize high efficient polarization control [11].

The general constitutive relations of the bianisotropic MMs are expressed as $\bar{D} = \epsilon_0 \bar{\epsilon}_r \cdot \bar{E} + ic^{-1} \bar{\chi} \cdot \bar{H}$ and $\bar{B} = \mu_0 \bar{\mu}_r \cdot \bar{H} - ic^{-1} \bar{\chi}^T \cdot \bar{E}$, with $c = 1/\sqrt{\epsilon_0 \mu_0}$ being the velocity of light in the free space. The tensor $\bar{\chi}$ represents the magneto-electric (ME) polarization inside the medium, which in principle may

Received 15 April 2017, Accepted 27 May 2017, Scheduled 11 June 2017

* Corresponding author: Liang Peng (pengl@hdu.edu.cn).

¹ Key Laboratory for RF Circuits and Systems, Hangzhou Dianzi University, Ministry of Education, Hangzhou 310018, China.

² School of Optical and Electronic Information, Huazhong University of Science and Technology, Wuhan 430074, China.

hybridize the polarization. For instance, from [9] and [10], in forming the pseudo-spins, the constitutives of the constituting material take the form of $\bar{\epsilon} = \text{diag}[\epsilon_x, \epsilon_y, \epsilon_z]$, $\bar{\mu} = \text{diag}[\mu_x, \mu_y, \mu_z]$ and

$$\bar{\chi} = \begin{bmatrix} 0 & \chi_{xy} & 0 \\ \chi_{yx} & 0 & 0 \\ 0 & 0 & 0 \end{bmatrix}. \quad (1)$$

The existence of this kind of bianisotropy has been mentioned in composites without geometry symmetry, thus the ME effect is generally weak [12]. To obtain strong bianisotropy, the design of MMs with strong ME coupling turns out to be essential. For example, the achievement of enhanced bianisotropy is shown in Ref. [8, 10, 13], by embedding of split-ring resonators (SRRs) and/or Ω shaped resonators. Meanwhile, the effective parameter retrieval approach for one-dimension bianisotropic MMs is proposed as well [14, 15]. An alternative approach to obtain strong bianisotropy is to apply the high order modes of guidance system [16]. However, in all the above literatures, the realization of such bianisotropy requests the complex structures in three dimensions, which are hardly implemented through the standard planar lithography.

In this paper, we start from the construction and the homogenization of bianisotropic MMs by means of planar split-ring resonators (PSRRs). By building up the ME resonances from different orientated PSRRs, we give a systematic description of bianisotropic MM with arbitrary off-diagonal elements in $\bar{\chi}$. To meet the flexible implementation of such bianisotropy, we propose a 3D MM structure with strong bianisotropy, via a layer-by-layer configuration, with the desired ME resonance being maintained. As such, the proposed bianisotropic MMs would be realizable through the standard planar lithography. The justification of homogenization for the proposed MM is discussed, and our conclusion will be given.

2. BIANISOTROPIC MMS WITH INCLUSIONS OF PSRRS

From Eq. (1), bianisotropy means the existence of ME effect, i.e., \bar{E} and \bar{H} are directly coupled. If we look into a single unit cell of a typical MM consisting of wire and SRR, as shown in Fig. 1(a), the electric and magnetic responses are mainly determined by the two basic constituents, respectively. Being an isolated resonator with high quality (Q-factor), the SRR may be hardly influenced by its pitch. Due to current flowing on the SRR loop, the effective polarization can be obtained by averaging the flowing current intensity, while the effective magnetization would be obtained through integrating the rotation of the current flow.

In the study of the ME resonances, the electric and magnetic responses should be taken into account simultaneously. One can induce coupling between polarization (electric) and magnetization (magnetic) by breaking geometric symmetry of the unit cell. For instance, the SRR would be magnetized in case the wire is polarized, as shown in Fig. 1(a). A simpler example would be the unbalanced SRR shown in Fig. 1(b), where the ME coupling takes effect between E_z and H_y , hence χ_{zy} would be non-zero intrinsically. Technically, the polarization and the magnetization would be tuned by changing the width of the open cut on the SRR, which is labeled as d in Fig. 1(b). From the macroscopic point of view, if we treat the array of the unbalanced SRRs as an effective medium, the effective parameters may take the form of [8]

$$\epsilon_z = 1 + \frac{NA}{\omega_0^2 - \omega^2 + i\Gamma\omega}, \quad \mu_y = 1 + \frac{NB\omega^2}{\omega_0^2 - \omega^2 + i\Gamma\omega} \quad \text{and} \quad \chi_{zy} = \frac{ND\omega}{\omega_0^2 - \omega^2 + i\Gamma\omega}, \quad (2)$$

where ω_0 is the resonant frequency of the SRR; N is the density of SRRs; A, B, D are the coefficients determined by the SRR dimensions, while Γ represents the inevitable loss. We see that the dispersion of the effective parameters are not independent and can be tuned simultaneously. Numerical evaluation and validation of these parameters may be found in the rest part of the paper.

It is obvious that the orientation of the SRR is rotated, and the non-zero element in $\bar{\chi}$ changes as well. However, because only one element of $\bar{\chi}$ is involved by a single PSRR, a complicated $\bar{\chi}$ requests the combination of multiple PSRRs with different orientations. In Fig. 1(c) and Fig. 1(d), two perpendicular PSRRs are combined to achieve non-zero χ_{xy} and χ_{yx} . We emphasize that since the planar SRR can only link the ME response between perpendicular E and H , only the off-diagonal elements in $\bar{\chi}$ are involved by such kind MMs.

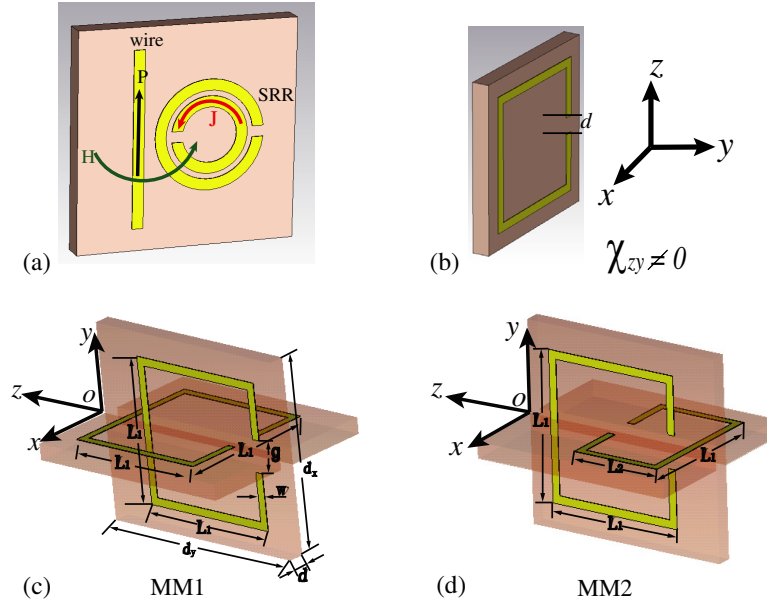


Figure 1. (color online) (a) MM unit cell composed of wire and SRR. (b) Non-zero elements of $\bar{\chi}$ involved by unbalanced SRRs with different orientations. (c) and (d) The composition of two perpendicular PSRRs. A couple of elements in $\bar{\chi}$ are non-zero. Please note the difference between these two structures.

3. BIANISOTROPY OF LAYERED STRUCTURES

As we see from the previous part, for a complex $\bar{\chi}$, multiple PSRRs with different orientations are needed. Although the complex structure shown in Figs. 1(c), (d) may be designed and fabricated in the microwave range, it is difficult to be adopted in the optical range through standard planar lithography. It is interesting but challenging to fabricate bianisotropic MMs desired by the PTIs on a planar substrate.

We go back to the standard SRR, which is redrawn in Fig. 2(a). In the physical model, ME resonance is realized by breaking the symmetry of the whole structure. The field distribution in resonance is also exhibited. It is obvious that the capacitance is brought by the two branches of the SRR. As the length of two branches is reduced, the capacitance is decreased. To preserve the capacitance, the dielectric constant in the host region is lifted up as ϵ_1 , see Fig. 2(b). We note that the shrinking of the branches degrades the asymmetry of the structure, thus suppress the ME coupling. To overcome this drawback and enhance the ME coupling, the permittivity of the branch region ϵ_2 is set to be higher than ϵ_1 . As such, the two branches may be totally taken away, with both the resonance and the ME coupling maintained, see Fig. 2(c). Consequently, the bianisotropic inclusion is transformed to a multi-layered structure, which may be conveniently implemented through the planar techniques. For the bianisotropic MMs shown in Fig. 1(c) and Fig. 1(d), their multi-layer counterparts are shown in Fig. 2(d) and Fig. 2(e). In the design, we assume the planar metallic structure is fabricated on a finite cylinder (ϵ_2) with radius r and height h , and both of the metals and the cylinders are embedded in the host background of ϵ_1 .

4. EFFECTIVE PARAMETERS USING RETRIEVAL PRINCIPLE

For homogeneous MMs, the effective parameters are crucial in determining their macroscopic EM responses. However, due to the resonance of the constituents, the effective parameters are hardly validated through traditional mixing theory [17]. The proper way to evaluate the MM's effective constitutives would be the retrieval approach with reflection and transmission by a MM slab [14].

The general wave solution inside the bianisotropic MM may be obtained through the approach

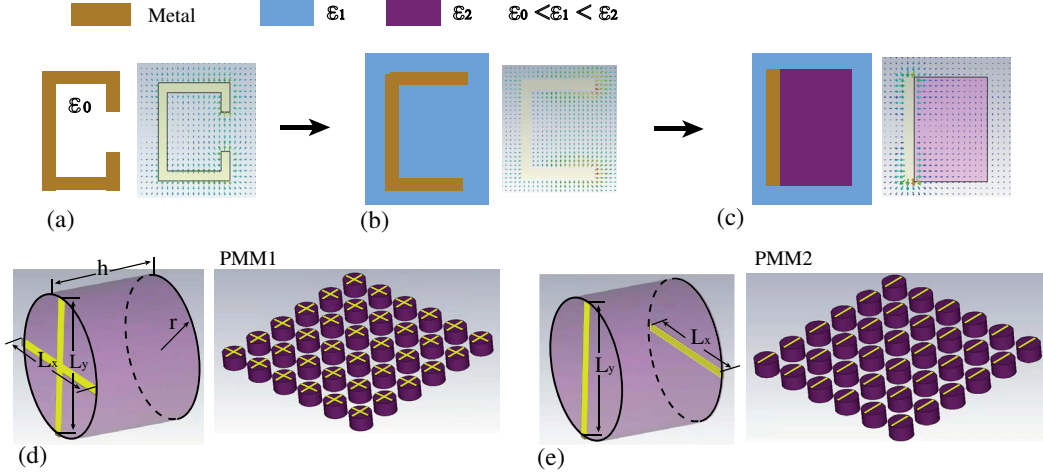


Figure 2. (color online) (a), (b) and (c) 3D to 2D deforming of bianisotropic MMs. (a) The PSRR is embedded inside the host of ϵ_0 ; (b) PSRR with branches being reduced, the host dielectric is ϵ_1 ($> \epsilon_0$); (c) Short metal wire without branch. The resonance is maintained by adding supplemental bulk with ϵ_2 ($> \epsilon_1$); the ME effect is realized by breaking the symmetry of the composite. (d) and (e) Two MMs made of planar composite with bianisotropy drastically different. In designing the two MMs, the thickness of the metal strip is 0.1 mm, the background has a dielectric constant of 2.4.

proposed in [18]. Here, we make the derivation further simplified. As we see in Fig. 1(c) and Fig. 1(d), the two SRRs are perpendicularly orientated. Depending on the incidence polarization, the wave propagation may be split into two cases, i.e., the decoupled TE and TM cases.

In order to find the effective parameters, we restrict ourselves to two particular propagations. Case I: $\vec{k} = \hat{y}k$; Case II: $\vec{k} = \hat{z}k$. In case I, TE plane waves ($\vec{E} = \hat{x}E$) would be influenced by μ_y , μ_z , ϵ_x and χ_{xy} , while TM plane waves ($\vec{H} = \hat{x}H$) would be influenced by ϵ_y , ϵ_z , μ_x and χ_{yx} , respectively. In case II, ϵ_x , μ_y and χ_{xy} are involved in the x -polarization, and ϵ_y , μ_x and χ_{yx} are involved in the y -polarization.

In case I, we assume $\vec{k} = \hat{y}k$, $\vec{E} = \hat{y}E_y + \hat{z}E_z$ and $\vec{H} = \hat{x}H$, then from Maxwell equations [20], we have

$$\hat{z}\omega^{-1}kH = \hat{y}\epsilon_0\epsilon_yE_y + \hat{z}\epsilon_0\epsilon_zE_z + \hat{y}ic^{-1}\chi_{yx}H, \quad (3)$$

$$\hat{x}\omega^{-1}kE_z = \hat{x}\mu_0\mu_xH - \hat{x}ic^{-1}\chi_{yx}E_y. \quad (4)$$

In these two equations, the time dependence $e^{-i\omega t}$ is omitted for time harmonic waves. It is a straight forward work to obtain

$$k^2 = k_0^2 \frac{\epsilon_z}{\epsilon_y} (\epsilon_y\mu_x - \chi_{yx}^2), \quad \frac{E_z}{H} = \frac{k}{\omega\epsilon_0\epsilon_z}, \quad \text{and} \quad \frac{E_y}{H} = \frac{-i\chi_{yx}}{\epsilon_0\epsilon_y c}, \quad (5)$$

with k_0 being the wave number in free space. If we define $\mu_{x,eff} = \frac{\epsilon_y\mu_x - \chi_{yx}^2}{\epsilon_y}$, then $k = k_0\sqrt{\epsilon_z\mu_{x,eff}}$, $\frac{E_z}{H} = \eta_0\sqrt{\frac{\mu_{x,eff}}{\epsilon_z}}$. Hence if there exists a MM slab in the free space, the reflection and transmission would be identical to that of an isotropic slab with ϵ_z and $\mu_{x,eff}$, since the normal component of E-field, i.e., E_y , will not affect the outcome by matching the continuity of tangential fields on the boundaries. Consequently, the effective parameters (ϵ_z and $\mu_{x,eff}$) would be extracted through the approach proposed in Ref. [14]. It is a similar process to retrieve μ_z and $\epsilon_{x,eff}$, the details are omitted.

In case II, we would first assume $\vec{E} = \hat{x}E$ and $\vec{H} = \hat{y}H$, since there is no coupling between the x and y components of E and H . From the source free Maxwell equations, we have

$$k^2 = k_0^2 (\epsilon_x\mu_y - \chi_{xy}^2), \quad \frac{E}{H} = \eta_0 \frac{kk_0^{-1} - i\chi_{xy}}{\epsilon_x} \quad \text{or} \quad \frac{E}{H} = \eta_0 \frac{\mu_y}{kk_0^{-1} + i\chi_{xy}}. \quad (6)$$

We see that the wave impedance (defined by $\frac{E}{H}$) is directionally dependant, i.e., it differs in case $k > 0$ and $k < 0$ [19]. This feature could help us to extract χ_{xy} from the full S matrix [15], which we show below.

Assume an MM slab with width d is placed in the free space, where the normal of the slab is in the z direction. An x polarized plane wave normally illuminates on the slab, then by matching the boundary conditions, one may derive the reflection (R) and transmission (T) from the slab. A standard deforming of the reflection and transmission may be found in [20]. Here we only show the relationship between R and T , which are

$$Te^{i(k_0+k)d} = 1 + R \frac{\eta_0 + \eta_+}{\eta_0 - \eta_+}, \quad (7)$$

$$\frac{1 + R - \eta_- \frac{1 - R}{\eta_0}}{1 - \frac{\eta_-}{\eta_+}} = \frac{1 + R - Te^{i(k_0+k)d}}{1 - e^{2ik_1d}}, \quad (8)$$

$$1 - \frac{\frac{-\eta_-}{\eta_+} + e^{2ik_1d}}{1 + \frac{-\eta_-}{\eta_+}} + \frac{1 - e^{2ik_1d}}{\frac{\eta_0}{-\eta_-} + \frac{\eta_0}{\eta_+}} = R \left[\frac{\frac{-\eta_-}{\eta_+} + e^{2ik_1d}}{1 + \frac{-\eta_-}{\eta_+}} + \frac{1 - e^{2ik_1d}}{\frac{\eta_0}{-\eta_-} + \frac{\eta_0}{\eta_+}} - \frac{\eta_0 + \eta_+}{\eta_0 - \eta_+} \right]. \quad (9)$$

In the above expression, η_+ and $-\eta_-$ are the wave impedances inside the slab with $k > 0$ and $k < 0$, respectively. The final expressions of R and T are not shown here, since they are rather complicated. In fact, the effective parameters would be successfully retrieved through Eq. (7) and Eq. (8).

The ϵ_x , μ_y and χ_{xy} may be extracted by

$$\chi_{xy} = \frac{ik}{\omega} \left(\frac{\eta_- + \eta_+}{-\eta_- + \eta_+} \right), \quad (10)$$

$$\mu_y = (k + i\omega\chi_{xy}) \frac{\eta_+}{\omega}, \quad (11)$$

$$\epsilon_x = (k - i\omega\chi_{xy}) \frac{1}{\omega\eta_+}. \quad (12)$$

Hence the two key parameters are k and η_+ , which we have to find from the reflectance and transmittance. In engineering, the reflectance and transmittance could be well found from the scattering matrix, i.e., S_{11} or S_{22} for R, S_{21} or S_{12} for T. Notice that S_{11} and S_{22} may differ, so η_+ and η_- are reasonably obtained by using Eq. (7), then we get

$$\eta_+ = \eta_0 \frac{1 + S_{11} - S_{21}e^{i(k_0+k)d}}{1 - S_{11} - S_{21}e^{i(k_0+k)d}}, \quad (13)$$

$$-\eta_- = \eta_0 \frac{1 + S_{22} - S_{12}e^{i(k_0+k)d}}{1 - S_{22} - S_{12}e^{i(k_0+k)d}}. \quad (14)$$

Applying Eq. (8), together with Eq. (13) and Eq. (14), we obtain

$$\begin{aligned} & \frac{1 + S_{11} + (1 - S_{11}) \frac{1 + S_{22} - S_{12}e^{i(k_0+k)d}}{1 - S_{22} - S_{12}e^{i(k_0+k)d}}}{1 + S_{11} - S_{21}e^{i(k_0+k)d}} (1 - e^{2ikd}) \\ &= 1 + \left(\frac{1 + S_{22} - S_{12}e^{i(k_0+k)d}}{1 - S_{22} - S_{12}e^{i(k_0+k)d}} \right) \left(\frac{1 - S_{11} - S_{21}e^{i(k_0+k)d}}{1 + S_{11} - S_{21}e^{i(k_0+k)d}} \right). \end{aligned} \quad (15)$$

If we define $x = e^{ikd}$, the above equation is further simplified as

$$S_{12}x^2 - \left[e^{ik_0d} S_{12} \cdot S_{21} + e^{-ik_0d} \cdot (1 - S_{11} \cdot S_{22}) \right] x + S_{21} = 0. \quad (16)$$

From the realistic reasons, the justified x should satisfy $|x| \leq 1$, due to the inevitable loss. As a result, the wave number k would be solved from

$$kd = [\ln(x)/i \pm 2n\pi], \quad (17)$$

with n being an integer. For the ϵ_y , μ_x and χ_{yx} , the procedure of retrieval would be identical if the y -polarized plane wave is excited in the MM. It should be note that the parameters in Case I can also be extracted through the approach proposed, with assuming zero bianisotropy.

5. NUMERICAL EVALUATION OF THE EFFECTIVE PARAMETERS

In this part, with the aid of computer based simulation, the effective parameters of two kind bianisotropic MMs are retrieved and discussed.

We first assume two bianisotropic MMs made by the 3D inclusions, as shown in Figs. 1(c) and (d). In the design, metallic SRRs are fabricated on the 1 mm thick F4B substrate, whose dielectric constant is 2.65 with loss tangent 0.003. The size of the two SRRs in one inclusion is different, such that χ_{xy} differs from χ_{yx} . The dimensions of the SRRs are shown in Figs. 1(c) and (d), which are $d_x = 12$ mm, $d_y = 13.5$ mm, $g = 2$ mm, $w = 0.5$ mm, $L_1 = 9$ mm and $L_2 = 6$ mm. In the simulation, a slab containing one layer MM unit cells is illuminated by an x -polarized incident wave propagating along z axis. The simulated S -parameters are shown in Figs. 3(a) and (b). Accordingly, the effective ϵ_x , μ_y and χ_{xy} are extracted, as shown in Figs. 3(c)–(e). It is seen that the parameters obey the anomalous dispersion described by Eq. (2). By using a similar procedure for the y -polarized incident wave, we would also work out ϵ_y , μ_x and χ_{yx} , respectively. Since both the simulated S parameters and the extracted effective parameters would be similar to the x polarized case, the results are omitted here.

Secondly, two bianisotropic MMs made of multi-layered composite are designed and simulated. The basic structures of the composites are shown in Figs. 2(d) and (e). In the simulation, we assume $\epsilon_1 = 2.4$, $\epsilon_2 = 12$, $r = 5$ mm and $h = 8$ mm. In both of the designs, $L_x = 10$ mm, $L_y = 8$ mm, and the periodicity in each of the x , y and z directions is 12 mm. Illuminated by an x polarized plane wave, the S -parameters for one layer structure and the extracted effective parameters (ϵ_x , μ_y and χ_{xy}) are shown

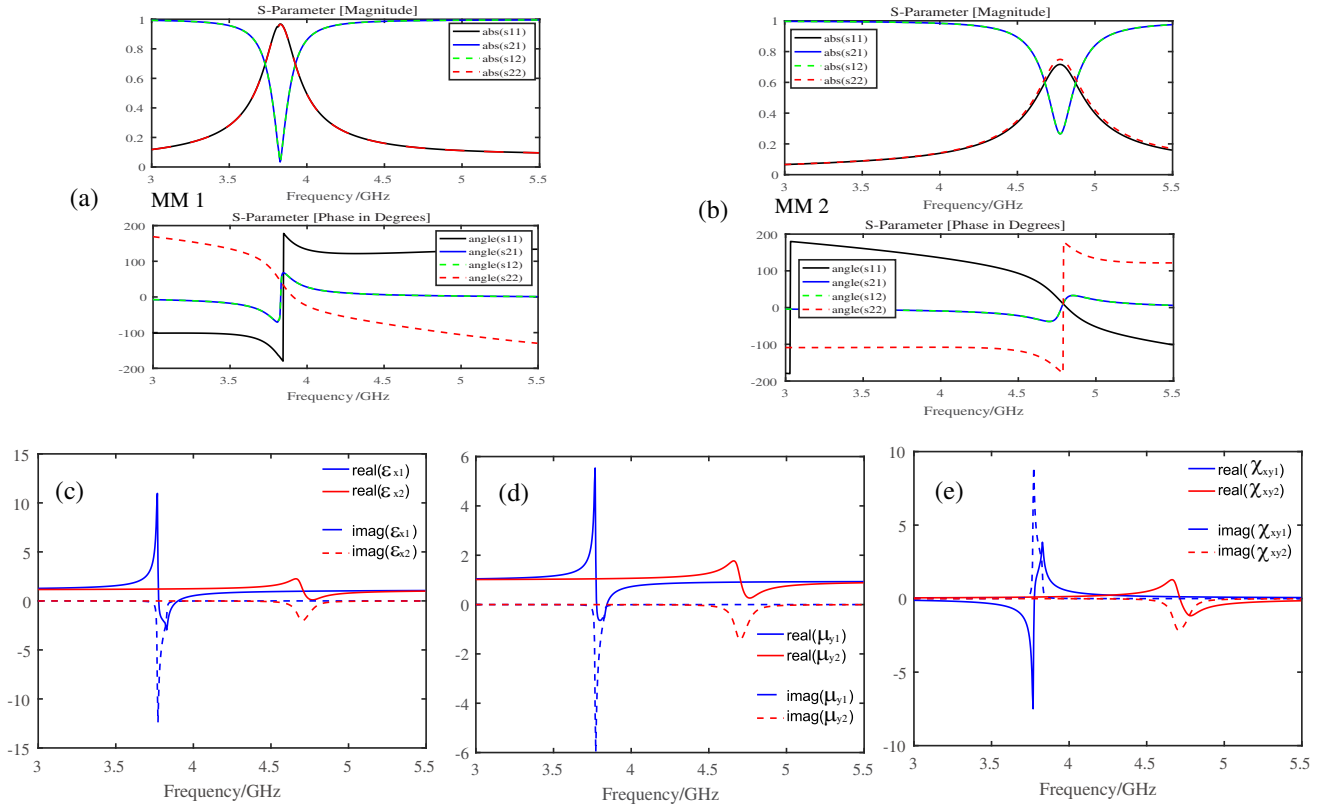


Figure 3. (color online) The simulated S parameters for the two MMs in Fig. 1(c), (d). (a) and (b) The full S parameters under x polarized incidence. (c)–(e) Retrieved ϵ_x , μ_y and χ_{xy} .

in Fig. 4. It is seen that the layered structure behaves identically to the metallic counterpart. The same procedure can be applied to the rest parameters, which are not shown here.

6. DISCUSSIONS

The homogenization of the MM is valid, provided that the dimension of a single unit cell is much smaller than λ_0 and/or λ_{eff} , with $\lambda_0(\lambda_{eff})$ being the free space wavelength(the effective wavelength) inside the MM. A typical size of the metallic unit cell would be $\frac{1}{6}\lambda_0$ [21]. As we see from Fig. 1, the size of the unit cell is 13.5 mm, which is in a range from $\frac{1}{7}\lambda_0$ to $\frac{1}{4}\lambda_0$ in the frequency band of interest. From Fig. 3, the retrieved ϵ and μ disperse a little bit, except those frequencies where the anomaly occurs, so that the homogenization in the metallic cases would be justified. It is similar to the layered MMs in Fig. 2, whose unit cell size is no larger than $\frac{1}{4}\lambda_0$, and the extracted parameters shown in Fig. 4 are also reasonable according to the previous theoretical model. So the homogenization is also valid.

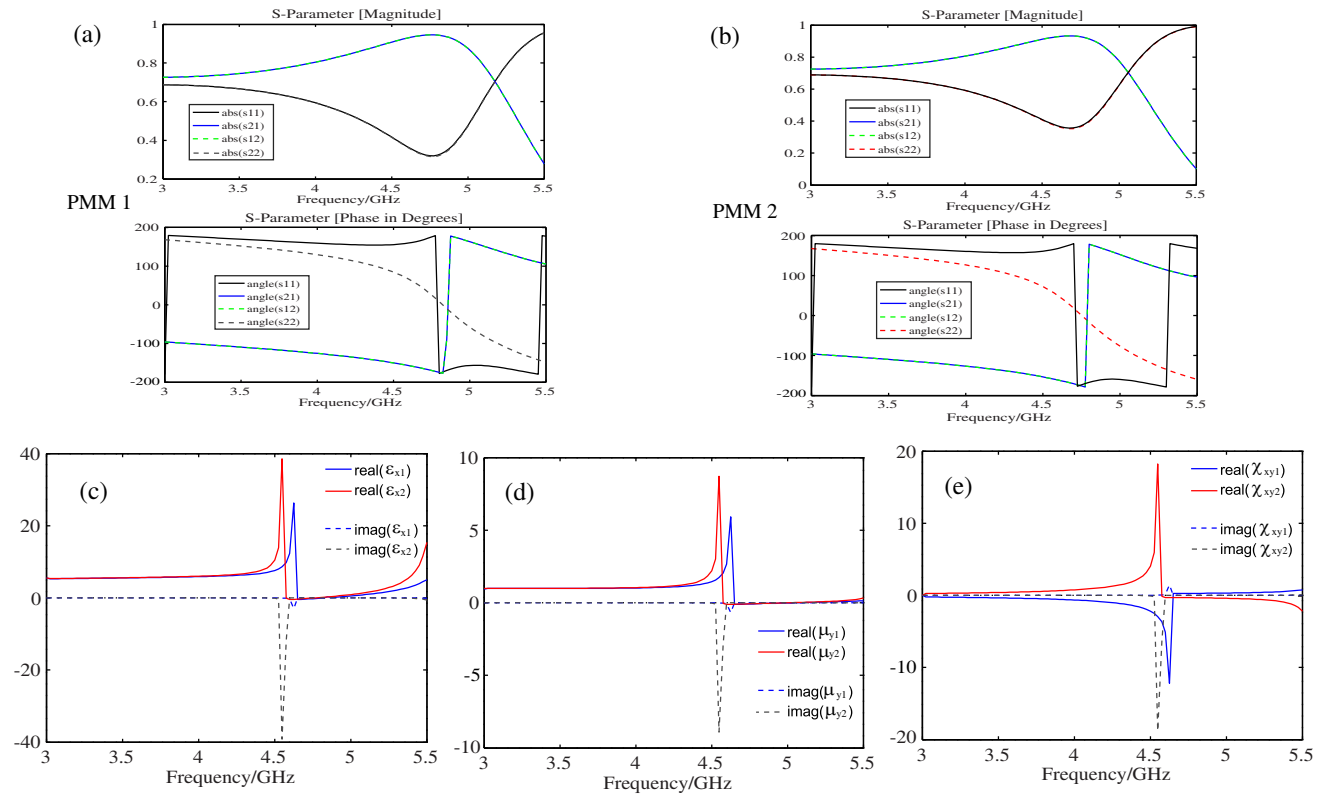


Figure 4. (color online) The simulated S parameters for the two MMs in Fig. 2(d)–(e). (a) and (b) The full S parameters under x polarized incidence. (c)–(e) Retrieved ϵ_x , μ_y and χ_{xy} . It is seen that the effective parameters are causal, but strongly affected by the periodic coupling (Bloch scattering) in the anomalous region.

It is worthy to mention that the effective wavelength is comparable to the unit cell size, close to the anomalous region, particularly for the layered inclusions. For the MMs with strong bianisotropy, this issue would be crucial, because the ME effect has to be enhanced through the resonance of the unit structures, which may make the homogenization fail. Numerically, the effective parameters is successfully extracted from the S -parameters. And mathematically, the curves shown in Fig. 3 and Fig. 4 are reasonable and causal. Although the coupling between adjacent structures may dominate the EM response inside the MM, the physical meaning of the parameters in the anomalous region would be justified by establishing a macroscopic potential model [22]. In such a case, the MM may be spatially dispersive, which could be treated as a photonic crystal as well.

For the effective ϵ_z and μ_z , we would assume the plane wave is z polarized (or z magnetically polarized). Then the retrieval would be completed by applying the S parameters through method proposed by Chen [14]. However, since the unit structure is not infinitesimal, these two parameters would be somehow influenced if \bar{k} varies, i.e., in case $\bar{k} = \hat{x}k$ or $\bar{k} = \hat{y}k$, ϵ_z and μ_z would be affected by resonance of χ_{xy} or χ_{yx} . Since the resonance of the ME resonator does not make sense to ϵ_z and μ_z , this effect may influence the effective parameters slightly and would not alternate the validation of the homogenization.

7. CONCLUSIONS

In conclusion, we systematically discuss the ME effect in MMs made of unbalanced PSRRs. The way to achieve different bianisotropy is given through comprehensive study. Because the planar structure can only connect the perpendicular electric and magnetic fields, the bianisotropic MMs discussed in this paper can only have non-zero off-diagonal elements in $\bar{\chi}$. To facilitate the bianisotropic MM through the planar lithography, we propose an approach to converted the corresponding 3D structure to a layer-by-layer counterpart, which behaves identically to the complex metallic structure. The justification and homogenization of the proposed MMs are verified with the aid of effective parameter retrieval, i.e., in our design, the unit cell is small enough, and the dispersive effective parameters are causal. Although influenced by the periodic effect, the retrieved parameters still show their justification and validation in the band of interest. Our method and retrieval algorithm are quite general and can be applied in improving some other designs, such as the Terahertz metamaterials with bianisotropy made of fishnet structure through standard planar lithography [23, 24].

ACKNOWLEDGMENT

This work is financially supported by the National Natural Science Foundation of China (NSFC, grant no: 61372022) and Natural Science Foundation of Zhejiang Province (ZJNSF, grant no: LY13F010020).

REFERENCES

1. Smith, D. R. and N. Kroll, "Negative refractive index in left-handed materials," *Physical Review Letters*, Vol. 85, 2933, 2000.
2. Pendry, J. B., A. J. Holden, W. J. Stewart, and I. Youngs, "Extremely low frequency plasmons in metallic mesostructures," *Physical Review Letters*, Vol. 76, No. 25, 1996.
3. Pendry, J. B., A. J. Holden, D. J. Robbins, and W. J. Stewart, "Magnetism from conductors and enhanced nonlinear phenomena," *IEEE Trans. Microwave Theory Tech.*, Vol. 47, 2075, 1999.
4. Veselago, V. G., "The electrodynamics of substances with simultaneously negative values of ϵ and μ ," *Sov. Phys. Usp.*, Vol. 10, 509, 1968.
5. Pendry, J. B., "Negative refraction makes a perfect lens," *Physical Review Letters*, Vol. 85, No. 18, 2000.
6. Pendry, J. B., D. Schurig, and D. R. Smith, "Controlling electromagnetic fields," *Science*, Vol. 312, 1780, 2006.
7. Liu, R., C. Ji, J. J. Mock, J. Y. Chin, T. J. Cui, and D. R. Smith, "Broadband ground-plane cloak," *Science*, Vol. 323, 366, 2009.
8. Khanikaev, A. B., S. H. Mousavi, W. K. Tse, M. Kargarian, A. H. Macdonald, and G. Shvets, "Photonic topological insulators," *Nature Materials*, Vol. 12, 233, 2013.
9. Chen, W. J., S. J. Jiang, X. D. Chen, B. Zhu, L. Zhou, J. W. Dong, and C. T. Chan, "Experimental realization of photonic topological insulator in a uniaxial metacrystal waveguide," *Nature Communications*, Vol. 5, 5782, 2014.
10. Guo, Q., W. Gao, J. Chen, Y. Liu, and S. Zhang, "Line degeneracy and strong spin-orbit coupling of light with bulk bianisotropic MMs," *Physical Review Letters*, Vol. 115, 067402, 2015.

11. Xu, J., B. Wu, and Y. Chen, "Elimination of polarization degeneracy in circularly symmetric bianisotropic waveguides: a decoupled case," *Optics Express*, Vol. 23, 11566, 2015.
12. Serdyudov, A., I. Semchenko, S. Tretyakov, and A. Sihvola, *Electromagnetics of Bi-anisotropic Materials: Theory and Applications*, Gordon and Breach Science Publishers, Amsterdam, 2001.
13. Slobozhanyuk, A. P., A. B. Khanikaev, D. S. Filonov, D. A. Smirnova, A. E. Miroshnichenko, and Y. S. Kivshar, "Experimental demonstration of topological effects in bianisotropic MMs," *Scientific Reports*, Vol. 6, 22270, 2016.
14. Chen, X., T. M. Grzegorzcyk, B.-I. Wu, J. J. Pacheco, and J. A. Kong, "Robust method to retrieve the constitutive effective parameters of MMs," *Physical Review E*, Vol. 70, 016608, 2004.
15. Li, Z., K. Aydin, and E. Ozbay, "Retrieval of effective parameters for bianisotropic MMs with omega shape metallic inclusions," *Photonics and Nanostructures-Fundamentals and Applications*, Vol. 10, 329, 2012.
16. Chen, W. J., S. J. Jiang, X. D. Chen, B. Zhu, L. Zhou, J. W. Dong, and C. T. Chan, "Experimental realization of photonic topological insulator in a uniaxial metacrystal waveguide," *Nature Communications*, Vol. 5, 5782, 2014.
17. Sihvola, A., *Electromagnetic Mixing Formulas and Applications*, IEE, London, 1999.
18. Grzegorzcyk, T. M., X. Chen, J. J. Pacheco, J. Chen, B.-I. Wu, and J. A. Kong, "Reflection coefficients and GOOS-Hänchen shifts in anisotropic and bianisotropic left-handed MMs," *Progress In Electromagnetics Research*, Vol. 51, 83, 2005.
19. Christine, É. K., M. S. Rill, S. Linden, and M. Wegener, "Bianisotropic photonic MMs," *IEEE Journal of Selected Topics in Quantum Electronics*, Vol. 16, 2, 2010.
20. Kong, J. A., *Electromagnetic Wave Theory*, EMW, Cambridge, MA, 2000.
21. Shelby, R. A., D. R. Smith, and S. Schultz, "Experimental verification of a negative index of refraction," *Science*, Vol. 292, 77–79, 2001.
22. Peng, L. and N. A. Mortensen, "Equal-potential interpretation of electrically induced resonances in MMs," *New Journal of Physics*, Vol. 13, 053012, 2011.
23. Kriegler, C. E., M. S. Rill, M. Thiel, E. Müller, S. Essig, A. Frölich, G. Freymann, S. Linden, D. Gerthsen, H. Hahn, K. Busch, and M. Wegener, "Transition between corrugated metal films and split-ring-resonator arrays," *Appl. Phys. B*, Vol. 96, No. 4, 749, 2009.
24. Rill, M. S., C. E. Kriegler, M. Thiel, G. Freymann, S. Linden, and M. Wegener, "Negative-index bianisotropic photonic MM fabricated by direct laser writing and silver shadow evaporation," *Optics Letters*, Vol. 34, No. 1, 19, 2009.